



Integral cross sections for electron impact excitation of vibrational and electronic states in phenol

R. F. C. Neves, D. B. Jones, M. C. A. Lopes, F. Blanco, G. García, K. Ratnavelu, and M. J. Brunger

Citation: *The Journal of Chemical Physics* **142**, 194305 (2015); doi: 10.1063/1.4921313

View online: <http://dx.doi.org/10.1063/1.4921313>

View Table of Contents: <http://scitation.aip.org/content/aip/journal/jcp/142/19?ver=pdfcov>

Published by the [AIP Publishing](#)

Articles you may be interested in

[Intermediate energy cross sections for electron-impact vibrational-excitation of pyrimidine](#)

J. Chem. Phys. **143**, 094304 (2015); 10.1063/1.4929907

[Intermediate energy electron impact excitation of composite vibrational modes in phenol](#)

J. Chem. Phys. **142**, 194302 (2015); 10.1063/1.4921038

[Differential cross sections for electron-impact vibrational-excitation of tetrahydrofuran at intermediate impact energies](#)

J. Chem. Phys. **142**, 124306 (2015); 10.1063/1.4915888

[Absolute cross sections for vibrational excitations of cytosine by low energy electron impact](#)

J. Chem. Phys. **137**, 115103 (2012); 10.1063/1.4752655

[Cross sections for electron impact excitation of the vibrationally resolved A \$\Pi\$ 1 electronic state of carbon monoxide](#)

J. Chem. Phys. **126**, 064307 (2007); 10.1063/1.2434169

The image shows the cover of an AIP Applied Physics Reviews journal. The cover features a blue and orange color scheme with a molecular structure in the background. The text 'AIP Applied Physics Reviews' is at the top left. The main title 'NEW Special Topic Sections' is in large white letters. Below it, the text 'NOW ONLINE' is in yellow, followed by 'Lithium Niobate Properties and Applications: Reviews of Emerging Trends' in white. The AIP Applied Physics Reviews logo is at the bottom right.

NEW Special Topic Sections

NOW ONLINE
Lithium Niobate Properties and Applications:
Reviews of Emerging Trends

AIP Applied Physics Reviews

Integral cross sections for electron impact excitation of vibrational and electronic states in phenol

R. F. C. Neves,^{1,2,3} D. B. Jones,¹ M. C. A. Lopes,³ F. Blanco,⁴ G. García,⁵ K. Ratnavelu,⁶ and M. J. Brunger^{1,6,a)}

¹School of Chemical and Physical Sciences, Flinders University, GPO Box 2100, Adelaide SA 5001, Australia

²Instituto Federal do Sul de Minas Gerais, Campus Poços de Caldas, Minas Gerais, Brazil

³Departamento de Física, Universidade Federal de Juiz de Fora, 36036-330 Juiz de Fora, Minas Gerais, Brazil

⁴Departamento de Física Atómica, Molecular y Nuclear, Universidad Complutense de Madrid, 28040 Madrid, Spain

⁵Instituto de Física Fundamental, CSIC, Serrano 113-bis, 28006 Madrid, Spain

⁶Institute of Mathematical Sciences, University of Malaya, 50603 Kuala Lumpur, Malaysia

(Received 23 March 2015; accepted 7 May 2015; published online 19 May 2015)

We report on measurements of integral cross sections (ICSs) for electron impact excitation of a series of composite vibrational modes and electronic-states in phenol, where the energy range of those experiments was 15–250 eV. There are currently no other results against which we can directly compare those measured data. We also report results from our independent atom model with screened additivity rule correction computations, namely, for the inelastic ICS (all discrete electronic states and neutral dissociation) and the total ionisation ICS. In addition, for the relevant dipole-allowed excited electronic states, we also report f -scaled Born-level and energy-corrected and f -scaled Born-level (BE f -scaled) ICS. Where possible, our measured and calculated ICSs are compared against one another with the general level of accord between them being satisfactory to within the measurement uncertainties. © 2015 AIP Publishing LLC. [<http://dx.doi.org/10.1063/1.4921313>]

I. INTRODUCTION

A significant effort has already been directed towards utilising atmospheric plasma treatment of biomass,^{1,2} in order to generate useful chemicals such as ethanol and phenol. In particular, phenol (C₆H₅OH) has been identified³ as a potential target of electron-induced breakdown of lignin (a phenolic-based moiety), and so, it represents an excellent prototype subunit for lignin. Phenol and its derivatives are often utilised or produced in industrial processes, often leading to their presence in wastewater.⁴ The high toxicity, persistence, and suspected mutagenicity/carcinogenicity of phenols (particularly chloro/fluoro-phenols) suggest that they pose a serious threat to ecology and the environment.^{5,6} Plasmas have, therefore, also been investigated to remove phenolic based species from wastewater as a remediation strategy.^{7–10} In order to gain a fundamental understanding for the utility of atmospheric plasmas to economically produce bio-fuels and other useful chemicals, or degrading toxic compounds, plasma simulations incorporating complete cross section databases (in fact, this is true in modelling most phenomena^{11–18}) are required. To this end, we have conducted a series of joint experimental and theoretical studies looking at the behaviour of electron–phenol scattering processes. Specifically, results for phenol's ($e, 2e$) triple differential cross sections (DCSs),¹⁹ elastic scattering and total cross sections (TCS),²⁰ vibrational excitation differential cross sections,²¹ and excited electronic-state differential cross sections²² have all thus far been reported. In addition,

the vibrational-mode and electronic-state spectroscopies of phenol have also been studied.^{21,23} Nonetheless, when simulating atmospheric plasma behaviour, etc., it is actually the integral cross sections (ICSs) (and the momentum transfer cross section) that are of most relevance to the modelling communities.^{11–18} As a consequence, in this short paper, we report on our derivation of vibrational-mode and electronic-state ICSs from our previously published differential cross section measurements.^{21,22}

Phenol also possesses a range of physico-chemical properties which, from our experience with other collision systems,^{24–30} are anticipated to play important roles in its scattering dynamics. Specifically, phenol has a permanent dipole moment of magnitude ~ 1.42 D³ and a significant average dipole polarisability of 10.53 Å³.³ We were therefore interested to see how those physico-chemical properties manifested themselves, if at all, in the behaviour of the measured composite vibrational-mode and/or electronic-state excitation ICSs. In addition, Neves *et al.*²¹ found some evidence for a higher-lying shape resonance enhancing the phenol cross sections *vis à vis* those of benzene. Support for the existence of that resonance was also found in our Schwinger Multichannel Method with Pseudo-potentials (SMCPP) calculations for the elastic channel²⁰ and our experimental total cross section measurements.²⁰ As the decay of a resonance into a given scattering channel or channels is often most easily seen through the measurements of excitation functions or integral cross sections,³¹ we were thus also interested to see if the proposed resonance manifested itself in our vibrational-mode and electronic-state ICSs.

The structure of the remainder of this paper is as follows. In Sec. II, we briefly describe our procedure for deriving ICSs

^{a)} Author to whom correspondence should be addressed. Electronic mail: Michael.Brunger@flinders.edu.au

TABLE I. Present experimental integral cross sections ($\times 10^{-20}$ m²) and related uncertainty (%) for electron impact excitation of the vibrational features in phenol.

Feature	15 eV		20 eV		30 eV		40 eV	
	ICS	Uncertainty	ICS	Uncertainty	ICS	Uncertainty	ICS	Uncertainty
Ring puckering +								
CO stretch + CC stretch	7.89	48%	1.76	52%	1.22	54%	1.18	62%
CH stretch + combination	3.10	48%	0.23	47%	0.071	50%	0.074	54%
OH stretch + combination	1.01	49%	0.07	54%	0.014	73%	0.009	79%
2 \times CH stretch	0.90	52%	0.023	69%	0.008	80%	0.007	83%

from our DCS measurements,^{21,22} as well as our independent atom model with screened additivity rule (IAM-SCAR) computations. References to relevant papers describing how our f -scaled Born-level and energy-corrected and f -scaled Born-level (BE, f -scaled) dipole-allowed ICS were determined are also given in this section. Thereafter, in Sec. III, our ICS results are presented and discussed before some conclusions arising from the present investigation are given in Sec. IV.

II. ANALYSIS PROCEDURES AND THEORY

All details pertaining to the composite vibrational-mode spectroscopy²¹ and excited electronic-state spectroscopy²³ of phenol can be found in those earlier publications, and so, we do not repeat them again here. Rather, we simply note that integral cross sections for the (i) ring puckering plus CO-stretch plus CC-stretch composite vibrational-modes, (ii) CH-stretch plus combination composite vibrational-modes, (iii) OH-stretch plus combination composite vibrational-modes, (iv) 2 \times CH-stretch overtone vibrational mode, (v) band 1 excited electronic-states, (vi) band 2 excited electronic-states, (vii) band 3 excited electronic-states, (viii) band 4 excited electronic-states, and (ix) band 5 excited electronic states

are reported in this paper. For the case of the vibrational excitation cross sections, whose data are summarised in Table I and plotted in Fig. 1, the incident electron energy range is 15–40 eV. On the other hand, the electronic-state excitation cross sections, which are listed in Table II and plotted in Fig. 2, cover the incident electron energy range from 15 to 250 eV.

A full description of our experimental and data analysis methodologies, in going from the measured electron energy loss spectra to deriving the absolute inelastic DCSs, can be found in Neves *et al.*^{21,22} (to whom the reader is referred for more details). The DCS (σ_i) for a given scattering process, i (in this case $i = (i)-(ix)$ above), is related to the ICS, Q_i , through the standard formula

$$Q_i(E_0) = 2\pi \int_0^\pi \sigma_i(E_0, \theta) \sin \theta d\theta, \quad (1)$$

where E_0 = incident electron energy and θ = scattered electron angle.^{28,30} In order to convert experimental DCS data, measured at discrete angles that span a finite angular range determined by the physical constraints of the apparatus, to an ICS, one must first extrapolate and interpolate the measured data so that they cover the full angular range from 0° to 180°. Our approach to accomplish this, built around a generalised

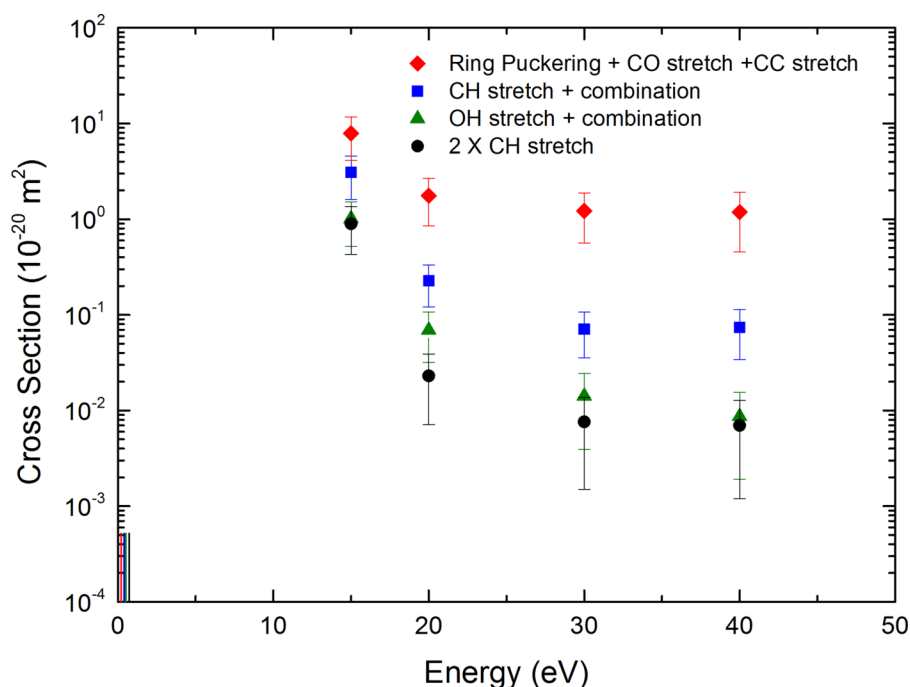


FIG. 1. Integral cross sections ($\times 10^{-20}$ m²) as a function of incident electron energy for excitation of the (a) ring puckering + CO stretch + CC stretch (red diamond), (b) CH stretch + combination (blue square), (c) OH stretch + combination (green triangle), and (d) CH stretch overtone (black circle) composite vibrational-modes in phenol. See also legend in figure.

TABLE II. Present experimental integral cross sections ($\times 10^{-20}$ m²) and related uncertainty (%) for electron impact excitation of the electronic-state features in phenol.

Feature	15 eV		20 eV		30 eV		40 eV		250 eV	
	ICS	Uncertainty	ICS	Uncertainty	ICS	Uncertainty	ICS	Uncertainty	ICS	Uncertainty
Band 1	0.55	60%	0.12	64%	0.04	64%	0.03	71%
Band 2	1.15	50%	0.37	55%	0.14	41%	0.12	44%	0.05	19%
Band 3	1.64	43%	0.62	49%	0.36	35%	0.35	33%	0.23	10%
Band 4	4.52	45%	2.21	46%	1.73	34%	1.52	32%	1.59	7%
Band 5	2.91	44%	0.79	53%	0.43	36%	0.41	36%
Sum	10.77	24%	4.11	28%	2.70	23%	2.43	22%	1.87	6%

oscillator strength (GOS) formalism³² for optically allowed states (there are many singlet electronic-states in bands 2, 3, and 4 that fulfil this criterion, while the main vibrational composite contributions come from the infrared active modes^{21,23}), has also been described in some detail previously²⁷ and so we do not repeat that detail here. As stated above, the present composite vibrational mode ICSs and their associated uncertainties are listed in Table I and plotted in Fig. 1, while the present excited electronic-state ICSs and their associated uncertainties are listed in Table II and Fig. 2. All the uncertainties are at the one standard deviation level and arise from the intrinsic errors on the measured DCS, as well as an additional contribution due to our interpolation/extrapolation GOS approach. When those factors are combined in quadrature, the errors on our ICS (see Tables I and II) are found to be in the range 7%–83%, the precise error depending on the inelastic channel in question with the highest uncertainties being found for band 1 (unresolved triplet) electronic-states and the CH-stretch overtone.

We have also previously described our IAM-SCAR computations many times,^{20,30,33–35} so that only a précis need be given here. Basically, an atomic optical potential scattering model calculates all the phase shifts for each of the atoms

that comprise the molecule in question (i.e., carbon, oxygen, and hydrogen for phenol). The molecular scattering amplitude then stems from the sum of all the relevant atomic amplitudes, including the phase coefficients. This is basically the so-called additivity rule (AR). However, the AR does not account for the target molecular structure, so that some screening coefficients (SCs) are also employed in order to account for the geometry of the molecule (atomic positions and bond lengths). With that approach, the IAM-SCAR has been known to provide a good description of the scattering process down to ~ 20 eV for some molecules.^{33–35} On the other hand, there are other systems^{36–38} where the IAM-SCAR approach results do not agree well with the measured cross sections at even 50 eV, so that caution in its application must still be exercised.

Finally, the determination of our f -scaled Born-level ICS and BE f -scaled ICS, for bands 2, 3, and 4 excited electronic-states in phenol, was performed using the procedures outlined in the papers by Kim and his colleagues^{39–41} with the results being plotted in Fig. 2. In essence, Jones *et al.*²³ determined $G_{\text{exp}}(K^2)$, where K^2 is the momentum transfer in the collision (see Eq. (4) in Kato *et al.*⁴⁰), for each of bands 2, 3, and 4, using a Vriens⁴² parameterisation. Now we, in turn, subsequently

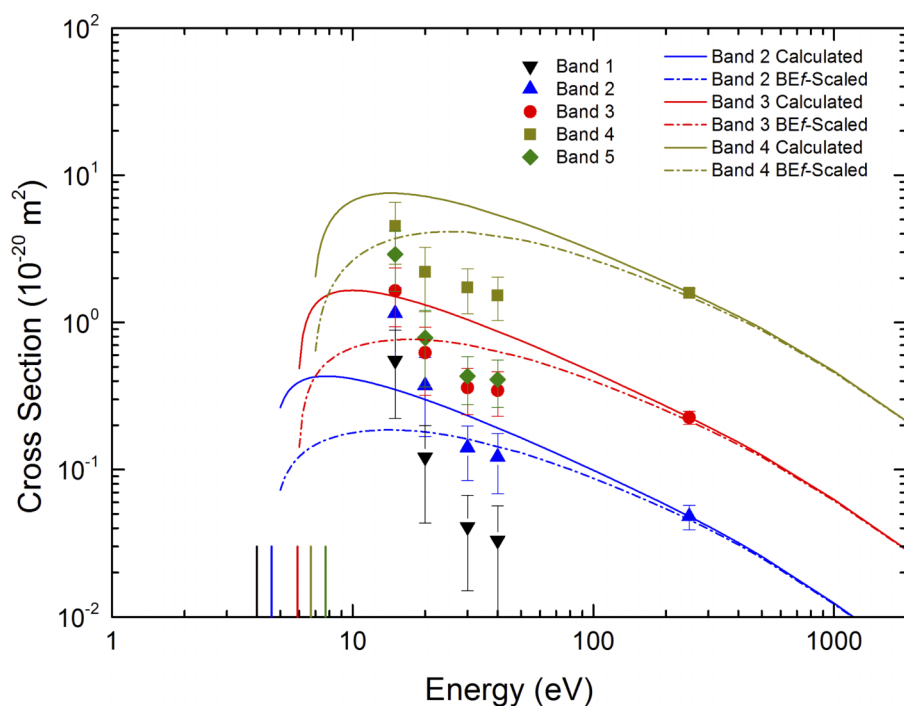


FIG. 2. Present integral cross sections ($\times 10^{-20}$ m²) for electron impact excitation of (a) band 1 (filled down triangle), (b) band 2 (blue triangle), (c) band 3 (red bullet), (d) band 4 (tan square), and (e) band 5 (seagreen diamond) electronic-states in phenol. Also shown are our various f -scaled Born-level (denoted as “calculated” in the legend) and BE f -scaled ICSs for the dipole-allowed transitions (bands 2, 3, 4) in phenol. See also legend in figure.

employed those $G_{\text{exp}}(K^2)$ in Eq. (10) of Kato *et al.*⁴⁰ to determine Q_{Born} for each band. However, as found by Jones *et al.*,²³ the optical oscillator strengths (f), as derived from the $G_{\text{exp}}(K^2)$ versus K^2 fits, were in excellent agreement in each case with those from corresponding independent determinations (both experimental and theoretical). As a consequence, the derived Q_{Born} are in fact equivalent to the f -scaled Born cross sections of Eq. (1) in Kato *et al.*⁴⁰ Next, we apply the energy-scaling correction, which corrects the deficiency of the Born approximation at lower E_0 without losing its well-known validity at high E_0 , to ultimately determine the BE f -scaling ICSs of each band (see Eq. (3) in Kato *et al.*⁴⁰).

III. RESULTS AND DISCUSSION

If we now consider Fig. 1, which plots all our composite vibrational-mode ICSs (see also Table I), then it should be immediately apparent that there are no other experimental measurements nor theoretical calculations against which we can compare the present results. Of course, in terms of theory, such calculations would involve moving away from the fixed-nuclei approximation, and for a relatively complicated molecule like phenol, this would be a significant challenge. From the experimental side, we would welcome and encourage cross check measurements from other active groups. Please note that also shown in Fig. 1 are the threshold energies for each of the composite vibrational-modes investigated.²¹ Threshold energies are important quantities in simulation studies^{11–18} and as such are denoted here for information purposes. It is clear that the ICS energy dependencies, for each of the modes, are very similar, to within the errors quoted. We also find that the magnitude of the ICS for the ring puckering + CO-stretch + CC-stretch composite mode is larger than that for the CH-stretch + combination composite mode which is in turn greater than the ICS for the OH-stretch + combination composite modes that are larger in magnitude than the CH-stretch overtone (see Fig. 1). It is well known from infrared spectroscopy that the intensity of a fundamental mode is in general much larger than that for its overtone, with the results in Fig. 1 for the CH-stretch and CH-stretch overtone ($2 \times$ CH-stretch) being consistent with that observation. We had previously observed that there is some evidence, in our elastic cross section calculations^{3,20} and total cross section measurements,²⁰ for the existence of a broad shape resonance for incident electron energies in the ~ 10 – 20 eV range. Further support for this notion can be found in Fig. 1, where the ICS at 15 eV, and for each of the composite vibrational modes reported, increases significantly in magnitude compared to the trend in the cross sections for energies in the 20–40 eV regime. This effect is particularly prevalent when the shape resonance decays into the CH-stretch overtone. In Neves *et al.*,²¹ we found that the angular distributions (DCSs) for each of the composite modes typically became more forward peaked in magnitude as the incident beam energy (E_0) is increased. This is indicative for the effect that the dipole moment and dipole polarisability of phenol have on the scattering process and leads to somewhat higher magnitude ICS for the composite vibrational-modes at 30 eV and 40 eV than might otherwise be the case.

With respect to our ICSs for excitation of bands 1–5 electronic-states (see Fig. 2), we again find that there are no independent data against which we can compare the current results. In this case, however, we can compare our measured data against f -scaled Born ICSs and BE f -scaled ICSs that were determined as a part of the present study. Note that those Born results are only able to be calculated for optically allowed transitions and so are restricted to bands 2, 3, and 4 which consist of many dipole-allowed singlet states.^{22,23} However, as noted in Jones *et al.*,²³ there are also many optically forbidden triplet states in bands 2, 3, and 4 which make a comparison between our measured ICS and the Born-results for those bands of electronic-states a little problematic. Considering initially band 1 states, comprised of two unresolved triplets,²³ we find an almost typical energy dependence for excitation of optically forbidden states. Namely, a sharp on-set in the ICS near-threshold (inferred from Fig. 2) before the magnitude of the cross section decreases quite quickly with increasing E_0 as the exchange interaction becomes less important in the scattering dynamics. For band 2, containing a mixture of 2 singlet and 3 triplet states,²³ we find good agreement between our BE f -scaled ICS and the present measured ICS for $E_0 \geq 30$ eV (see Fig. 2). However, at $E \leq 20$ eV, the measured data are stronger in magnitude than calculated with the BE f -scaling approach. There are two possible causes for this observation. The first is the contribution of triplet-state “contamination” to the measured ICS as you go to energies close to threshold, while the second might be if the same shape resonance that decays into the elastic and vibrational channels were also to decay into the electronic-states. Note that the Born approach, by its very construction, cannot deal for the case where an incident electron is temporarily captured by a target species. Hence, we would not expect either the f -scaled Born or BE f -scaled ICS to be accurate under those circumstances. In the case of band 3, which is comprised of 4 triplet- and 4 singlet-states, we observe that only at 250 eV, where the triplet contributions are effectively zero to the ICS, is there good agreement between the Born ICSs and our measured ICSs (see Fig. 2). Note that the apparent agreement at 20 eV is, we believe, fortuitous with the intermediate energy BE f -scaling results tending to overestimate the magnitude of experimental band 3 ICS data and then underestimating it at 15 eV. A similar tale can also be gleaned from Fig. 2 in regards to band 4 excited electronic-states, which now consist of 10 singlet and 11 triplet states. However, in this case, there are two unresolved $^1A'$ electronic-states, with an optical oscillator strength of ~ 0.96 , that, on the basis of the energy-loss spectra in Jones *et al.*,²³ might *a priori* have been expected to dominate band 4 behaviour and so be amenable to being well described by a Born-level calculation. In fact, this is not what we find in Fig. 2 where the band 4 BE f -scaled ICS again overestimates the magnitude of the experimental results at intermediate energies. There are many cases, for isolated optically allowed states in relatively simpler molecular systems (e.g., CO,^{40,43} H₂,⁴⁴ CO₂,⁴⁵ and N₂O⁴⁶), where, away from resonances, the BE f -scaling approach has been demonstrated to provide a very good representation of the measured ICSs at energies $E_0 \geq 15$ eV. This is clearly not the case with phenol, where it appears to fail at intermediate energies for bands 3 and 4. Whether or

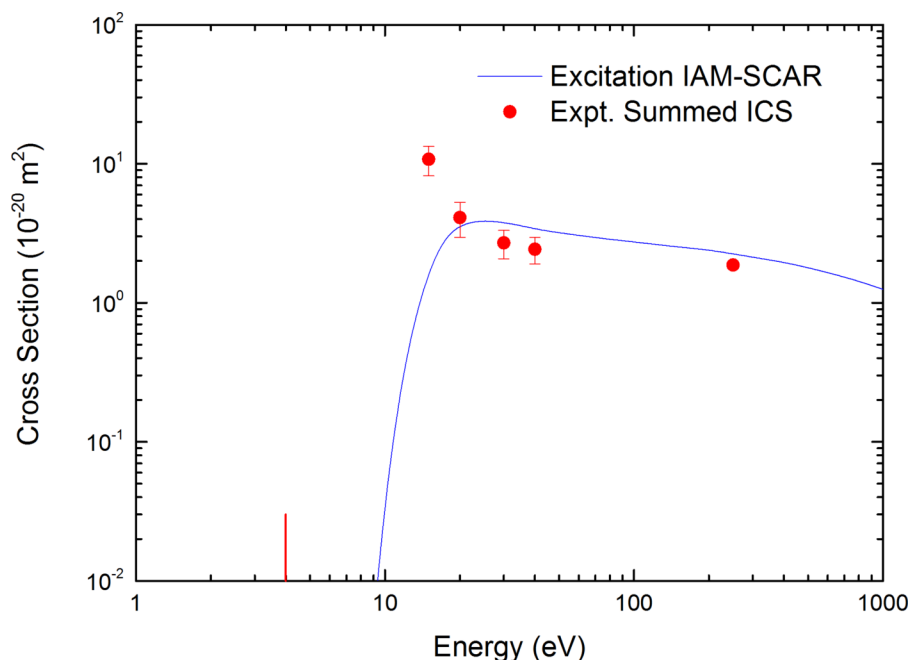


FIG. 3. Present (red bullet) summed (bands 1–5) electronic-state ICSs ($\times 10^{-20} \text{ m}^2$) for $e^- + \text{C}_6\text{H}_5\text{OH}$ scattering. Also shown is the corresponding electronic-state excitation and neutral dissociation ICS for phenol from our IAM-SCAR (blue solid line) calculations. See also legend in figure. The vertical red line indicates the known threshold energy for the electronic-states.²³

not this apparent failure is due to the quite detailed mixture of singlet and triplet states within bands 3 and 4, and some form of interchannel coupling going on between them,²⁰ or another reason, awaits a detailed *ab initio* theoretical analysis. Finally, in regards to band 5, we simply note that the energy dependence of its ICSs is very similar to that previously seen (see Fig. 2) for each of bands 2–4. This is perhaps not that surprising since it too is also a band comprised of a mixture of excited singlet- and triplet-electronic-states.²³

In Fig. 3, we now plot the sum of our bands 1–5 electronic-state ICSs (see also the foot of Table II for a listing of that data) and compare that to our IAM-SCAR result for “excitation” processes in phenol. In fact, the IAM-SCAR cross section represents not only the sum of all the electronic-states but also a contribution from the phenol neutral dissociation ICS. Note that the error bars plotted in Fig. 3 are all at the one standard deviation level and represent, at each E_0 , the quadrature sum of the absolute errors on the component ICSs for bands 1–5 that comprise that sum. A listing of those errors can also be found at the foot of Table II. It is clear from Fig. 3 that there is a quite good level of accord between the present summed ICS and the IAM-SCAR result, for $E_0 \geq 20$ eV, with the theory only being slightly stronger in magnitude over most of that common energy range. This suggests that the electron impact neutral dissociation cross section is actually relatively small. This is a particularly interesting result in elucidating the mechanism of benzyl radical production (C_6H_5), which is known to be important in plasmas produced from phenolic based species. It is therefore likely that the benzyl radical is produced through other mechanisms, such as dissociative electron attachment or dissociation following electron or photon-impact excitation. Of course, this level of agreement could be a little fortuitous, as the IAM-SCAR “excitation” threshold is clearly ~ 4 eV higher than the known physical threshold energy for excitation of the electronic-states in phenol (see Fig. 3). The other striking feature of Fig. 3 is the strength of the 15 eV summed ICS compared with the trend of the summed ICS values from 20 to

250 eV. This could well be further supportive evidence for the decay of a shape resonance, into one or more of those excited bands, around the 10–20 eV energy range.^{3,20} Certainly, this is a point that warrants further study. Finally, considering the results at 20 eV, we find that the summed electronic-state ICSs contribute $\sim 10\%$ of the grand total cross section²⁰ at that energy. This is quite an appreciable contribution; in our earlier work with α -tetrahydrofurfuryl alcohol at 20 eV, the electronic-state contribution to the TCS was only $\sim 1.7\%$. This result, particularly in relation to the modelling community, is an important one as it clearly suggests that the electronic-state contributions to the scattering can vary significantly from one molecule to the next and so must be considered on a molecule by molecule basis.

IV. CONCLUSIONS

We have reported on a series of integral cross section results, for electron impact excitation ($E_0 = 15\text{--}250$ eV) of some composite vibrational modes and bands of excited electronic-states in phenol. In general, there were no other experimental results against which we could benchmark our data, and for the particular cases of bands 2, 3, and 4 excited electronic-states, only Born-level theory was available to compare against. As one of the main aims of this study was to provide absolute cross sections that could be incorporated into simulations of atmospheric plasma action on biomass, we consider the present investigation to have been successful to some degree. Further work, however, is needed to push the available measurements closer to threshold and *ab initio* quality theory is needed in general for these systems. Nonetheless, if the present results were combined with our earlier work on elastic scattering, total momentum transfer cross sections, and total cross sections,²⁰ then a reasonable database starting point, for modelling applications in which phenol is a constituent, has probably been achieved.

ACKNOWLEDGMENTS

This work was supported by the Australian, Brazilian, and Spanish governmental funding agencies (ARC, CNPq, CAPES, and MINECO). D.B.J. thanks the ARC for a Discovery Early Career Researcher Award. R.F.C.N. acknowledges CNPq and Flinders University for financial assistance, while M.J.B. thanks CNPq for his “Special Visiting Professor” award and the University of Malaya for his “Distinguished Visiting Professor” award. M.C.A.L. acknowledges financial support from CNPq and FAPEMIG, while G.G. acknowledges financial support from MINECO (No. FIS2012-31230) and COST (Nos. MP1002 and CM1301).

- ¹J. Amorim, C. Oliveira, J. A. Souza-Corrêa, and M. A. Ridenti, *Plasma Processes Polym.* **10**, 670 (2013).
- ²E. M. de Oliveira, R. F. da Costa, S. d. A. Sanchez, A. P. P. Natalense, M. H. F. Bettega, M. A. P. Lima, and M. T. do N. Varella, *Phys. Chem. Chem. Phys.* **15**, 1682 (2013).
- ³E. M. de Oliveira, S. d. A. Sanchez, M. H. F. Bettega, A. P. P. Natalense, M. A. P. Lima, and M. T. do N. Varella, *Phys. Rev. A* **86**, 020701(R) (2012).
- ⁴V. A. Cooper and J. A. Nicell, *Water Res.* **30**, 954 (1996).
- ⁵I. Alemzadeh and S. Nejati, *J. Hazard. Mater.* **166**, 1082 (2009).
- ⁶A. Chen *et al.*, *Chemosphere* **109**, 208 (2014).
- ⁷B. P. Dojčinović, D. Manojlović, G. M. Roglić, B. M. Obradović, M. M. Kuraica, and J. Purić, *Vacuum* **83**, 234 (2009).
- ⁸B. Sun, M. Sato, and J. S. Clements, *Environ. Sci. Technol.* **34**, 509 (1999).
- ⁹H. Yang, G. Mengen, Y. Matsumoto, and M. Tezuka, *J. Environ. Sci.* **25**(Supplement 1), S180 (2013).
- ¹⁰S. Li, X. Ma, L. Liu, and X. Cao, *RSC Adv.* **5**, 1902 (2015).
- ¹¹L. Campbell and M. J. Brunger, *Plasma Sources Sci. Technol.* **22**, 013002 (2013).
- ¹²M. C. Fuss, A. G. Sanz, A. Muñoz, F. Blanco, M. J. Brunger, S. J. Buckman, P. Limão-Vieira, and G. García, *Appl. Radiat. Isot.* **83**, 159 (2014).
- ¹³R. D. White, W. Tattersall, G. Boyle, R. E. Robson, S. Dujko, Z. Lj. Petrovic, A. Bankovic, M. J. Brunger, J. P. Sullivan, S. J. Buckman, and G. García, *Appl. Radiat. Isot.* **83**, 77 (2014).
- ¹⁴N. A. Garland, M. J. Brunger, G. García, J. de Urquijo, and R. D. White, *Phys. Rev. A* **88**, 062712 (2013).
- ¹⁵R. D. White, M. J. Brunger, N. A. Garland, R. E. Robson, K. F. Ness, G. García, J. de Urquijo, S. Dujko, and Z. Lj. Petrović, *Eur. Phys. J. D* **68**, 125 (2014).
- ¹⁶A. G. Sanz, M. C. Fuss, A. Muñoz, F. Blanco, P. Limão-Vieira, M. J. Brunger, S. J. Buckman, and G. García, *Int. J. Radiat. Biol.* **88**, 71 (2012).
- ¹⁷K. F. Ness, R. E. Robson, M. J. Brunger, and R. D. White, *J. Chem. Phys.* **136**, 024318 (2012).
- ¹⁸J. de Urquijo, E. Basurto, A. M. Juárez, K. F. Ness, R. E. Robson, M. J. Brunger, and R. D. White, *J. Chem. Phys.* **141**, 014308 (2014).
- ¹⁹G. B. da Silva, R. F. C. Neves, L. Chiari, D. B. Jones, E. Ali, D. H. Madison, C. G. Ning, K. L. Nixon, M. C. A. Lopes, and M. J. Brunger, *J. Chem. Phys.* **141**, 124307 (2014).
- ²⁰R. F. da Costa, E. M. de Oliveira, M. H. F. Bettega, M. T. do N. Varella, D. B. Jones, M. J. Brunger, F. Blanco, R. Colmenares, P. Limão-Vieira, G. García, and M. A. P. Lima, *J. Chem. Phys.* **142**, 104304 (2015).
- ²¹R. F. C. Neves, D. B. Jones, M. C. A. Lopes, K. L. Nixon, E. M. de Oliveira, R. F. da Costa, M. T. do N. Varella, M. H. F. Bettega, M. A. P. Lima, G. B. da Silva, and M. J. Brunger, “Intermediate energy electron impact excitation of composite vibrational modes in phenol.” *J. Chem. Phys.* (in press).
- ²²R. F. C. Neves, D. B. Jones, M. C. A. Lopes, K. L. Nixon, G. B. da Silva, H. V. Duque, E. M. de Oliveira, R. F. da Costa, M. T. do N. Varella, M. H. F. Bettega, M. A. P. Lima, K. Ratnavelu, G. García, and M. J. Brunger, *J. Chem. Phys.* **142**, 104305 (2015).
- ²³D. B. Jones, G. B. da Silva, R. F. C. Neves, H. V. Duque, L. Chiari, E. M. de Oliveira, M. C. A. Lopes, R. F. da Costa, M. T. do N. Varella, M. H. F. Bettega, M. A. P. Lima, and M. J. Brunger, *J. Chem. Phys.* **141**, 074314 (2014).
- ²⁴T. P. T. Do, M. Leung, M. Fuss, G. García, F. Blanco, K. Ratnavelu, and M. J. Brunger, *J. Chem. Phys.* **134**, 144302 (2011).
- ²⁵D. B. Jones, S. M. Bellm, P. Limão-Vieira, and M. J. Brunger, *Chem. Phys. Lett.* **535**, 30 (2012).
- ²⁶D. B. Jones, S. M. Bellm, F. Blanco, M. Fuss, G. García, P. Limão-Vieira, and M. J. Brunger, *J. Chem. Phys.* **137**, 074304 (2012).
- ²⁷Z. Mašín, J. D. Gorfinkiel, D. B. Jones, S. M. Bellm, and M. J. Brunger, *J. Chem. Phys.* **136**, 144310 (2012).
- ²⁸H. V. Duque, L. Chiari, D. B. Jones, P. A. Thorn, Z. Pettifer, G. B. da Silva, P. Limão-Vieira, D. Duflot, M.-J. Hubin-Franskin, J. Delwiche, F. Blanco, G. García, M. C. A. Lopes, K. Ratnavelu, R. D. White, and M. J. Brunger, *Chem. Phys. Lett.* **608**, 161 (2014).
- ²⁹P. Limão-Vieira, D. Duflot, M.-J. Hubin-Franskin, J. Delwiche, S. V. Hoffmann, L. Chiari, D. B. Jones, M. J. Brunger, and M. C. A. Lopes, *J. Phys. Chem. A* **118**, 6425 (2014).
- ³⁰L. Chiari, H. V. Duque, D. B. Jones, P. A. Thorn, Z. Pettifer, G. B. da Silva, P. Limão-Vieira, D. Duflot, M.-J. Hubin-Franskin, J. Delwiche, F. Blanco, G. García, M. C. A. Lopes, K. Ratnavelu, R. D. White, and M. J. Brunger, *J. Chem. Phys.* **141**, 024301 (2014).
- ³¹M. J. Brunger and S. J. Buckman, *Phys. Rep.* **357**, 215 (2002).
- ³²E. N. Lassettre, *J. Chem. Phys.* **43**, 4479 (1965).
- ³³M. C. Fuss, A. G. Sanz, F. Blanco, J. C. Oller, P. Limão-Vieira, M. J. Brunger, and G. García, *Phys. Rev. A* **88**, 042702 (2013).
- ³⁴A. G. Sanz, M. C. Fuss, F. Blanco, J. D. Gorfinkiel, D. Almeida, F. Ferreira da Silva, P. Limão-Vieira, M. J. Brunger, and G. García, *J. Chem. Phys.* **139**, 184310 (2013).
- ³⁵H. Kato, A. Suga, M. Hoshino, F. Blanco, G. García, P. Limão-Vieira, M. J. Brunger, and H. Tanaka, *J. Chem. Phys.* **136**, 134313 (2012).
- ³⁶J. R. Brunton, L. R. Hargreaves, S. J. Buckman, G. García, F. Blanco, O. Zatsarinny, K. Bartschat, and M. J. Brunger, *Chem. Phys. Lett.* **568–569**, 55 (2013).
- ³⁷J. R. Brunton, L. R. Hargreaves, T. M. Maddern, S. J. Buckman, G. García, F. Blanco, O. Zatsarinny, K. Bartschat, D. B. Jones, G. B. da Silva, and M. J. Brunger, *J. Phys. B* **46**, 245203 (2013).
- ³⁸P. Palihawadana, J. P. Sullivan, S. J. Buckman, Z. Mašín, J. D. Gorfinkiel, F. Blanco, G. García, and M. J. Brunger, *J. Chem. Phys.* **139**, 014308 (2013).
- ³⁹Y.-K. Kim, *J. Chem. Phys.* **126**, 064305 (2007).
- ⁴⁰H. Kato, H. Kawahara, M. Hoshino, H. Tanaka, M. J. Brunger, and Y.-K. Kim, *J. Chem. Phys.* **126**, 064307 (2007).
- ⁴¹P. A. Thorn, M. J. Brunger, P. J. O. Teubner, N. Diakomichalis, T. Maddern, M. A. Bolorizadeh, W. R. Newell, H. Kato, M. Hoshino, H. Tanaka, H. Cho, and Y.-K. Kim, *J. Chem. Phys.* **126**, 064306 (2007).
- ⁴²L. Vriens, *Phys. Rev.* **160**, 100 (1967).
- ⁴³H. Kawahara, H. Kato, M. Hoshino, H. Tanaka, and M. J. Brunger, *Phys. Rev. A* **77**, 012713 (2008).
- ⁴⁴H. Kato, H. Kawahara, M. Hoshino, H. Tanaka, L. Campbell, and M. J. Brunger, *Phys. Rev. A* **77**, 062708 (2008).
- ⁴⁵H. Kawahara, H. Kato, M. Hoshino, H. Tanaka, L. Campbell, and M. J. Brunger, *J. Phys. B* **41**, 085203 (2008).
- ⁴⁶H. Kawahara, D. Suzuki, H. Kato, M. Hoshino, H. Tanaka, O. Ingólfsson, L. Campbell, and M. J. Brunger, *J. Chem. Phys.* **131**, 114307 (2009).